



Published in final edited form as:

J Med Chem. 2009 April 23; 52(8): 2443–2453. doi:10.1021/jm801556h.

Design and Synthesis of 2-Amino-4-methylpyridine Analogues as Inhibitors for Inducible Nitric Oxide Synthase and *in vivo* Evaluation of [¹⁸F]6-(2-Fluoropropyl)-4-methyl-pyridin-2-amine as a Potential PET Tracer for Inducible Nitric Oxide Synthase

Dong Zhou[†], Hsiaoju Lee[†], Justin M. Rothfuss[†], Delphine L. Chen[†], Datta E. Ponde^{†,‡}, Michael J. Welch[†], and Robert H. Mach^{†,*}

[†]Division of Radiological Sciences, Washington University School of Medicine, 510 South Kingshighway Boulevard, St. Louis, Missouri 63110

[‡]Current affiliate: Department of Radiology, University of Pennsylvania, 420 Curie Blvd, Philadelphia, PA 19104

Abstract

A series of position-6 substituted 2-amino-4-methylpyridine analogues was synthesized and compounds **9**, **18**, and **20** were identified as the inhibitors with the greatest potential to serve as PET tracers for imaging inducible nitric oxide synthase (iNOS). [¹⁸F]**9** was synthesized and evaluated in a mouse model of lipopolysaccharide (LPS)-induced iNOS activation. *In vivo* biodistribution studies of [¹⁸F]**9** indicate higher tracer uptake in the lungs of the LPS-treated mice when compared to control mice. Tracer uptake at 60 min post-injection was reduced in a blocking study using a known inhibitor of iNOS. The expression of iNOS was confirmed by Western blot analysis of lung samples from the LPS-treated mice. MicroPET studies also demonstrated accumulation of radiotracer in the lungs of the LPS-treated mice. Taken collectively, these data suggest that [¹⁸F]**9** shows favorable properties as a PET tracer to image iNOS activation with PET.

Introduction

Nitric oxide (NO) is an important and unique mediator of a variety of physiological and pathological processes.¹ NO is generated from the oxidation of L-arginine to L-citrulline in a two-step process by nitric oxide synthase (NOS) enzymes.² In the NOS family, there are two constitutive isozymes of NOS, neuronal NOS (nNOS) and endothelial NOS (eNOS), and one inducible isozyme (iNOS). The three isozymes of NOS are expressed in different tissues to generate NO for specific physiological roles. nNOS generates NO as a neurotransmitter and neuromodulator, mainly in brain and peripheral nerve cells; eNOS regulates blood pressure, primarily in vascular endothelial cells;³ iNOS is induced by various inflammatory stimuli (*e.g.* endotoxin) in activated macrophages and other types of cells and plays an crucial role in the host defense and the inflammatory processes.

Normally, the basal level of NO in all parts of the body is very low, mainly due to the constitutive nNOS and eNOS. In contrast, once expressed, iNOS can continue to generate NO

*Address correspondence to: Robert H. Mach, Ph.D. Division of Radiological Sciences Washington University School of Medicine Campus Box 8225 510 S. Kingshighway Blvd. St. Louis, MO 63110 e-mail: rhmach@mir.wustl.edu.

Supporting Information Available: Combustion analysis data of compound **9**, **11**, **13**, **15**, **16**, **18**, **20**, **24**, **27**, **30**, **33**, and **38**. This material is available free of charge via the Internet at <http://pubs.acs.org>.

in large amounts (up to μM concentrations) for a prolonged period of time.⁴ Studies have shown that production of NO by iNOS is implicated in a variety of acute and chronic inflammatory diseases (e.g., sepsis, septic shock, vascular dysfunction in diabetes, asthma, arthritis, multiple sclerosis and inflammatory diseases of the gut)⁵; iNOS activity has also been found in many tumors.⁶ Because of the central role of iNOS in NO-related diseases, numerous efforts have been made to develop iNOS inhibitors as pharmaceuticals ranging from the non-selective L-arginine analogues⁷ to the selective inhibitors reported recently.⁸ Some inhibitors of iNOS have shown promising results in animal models of sepsis, lung inflammation, arthritis, and autoimmune diabetes.^{8c} Therefore, the development of a radiolabeled iNOS inhibitor for probing iNOS expression *in vivo* using non-invasive positron emission tomography (PET) imaging will be of tremendous value to the study and treatment of NO-related diseases.

PET is being used more frequently in clinical and research studies because of its high sensitivity, good spatial resolution and ease in accurate quantification. Additionally, the absence of a physiologic effect from the radiotracers makes it a safe *in vivo* imaging tool. When short-lived positron-emitting radionuclides (^{18}F $t_{1/2} = 109.8$ min and ^{11}C $t_{1/2} = 20.4$ min) are incorporated into biologically active molecules (e.g. iNOS inhibitors), they can be used as tracers that target those physiological pathways. 2-amino-4-methylpyridine (**1**) has been reported as a non-selective NOS inhibitor with good potency;⁹ while the 6-substituted alkyl analogs of **1** have slightly improved potency and selectivity over the parent compound; analog **2** has the best potency (IC_{50} against iNOS = 28 nM).¹⁰ Computational calculations suggest that the position-6 is the most tolerant position to introduce a substituent¹¹ that would be suitable for radiolabeling with PET radionuclides ^{18}F and ^{11}C .

In the past decade, the development of radiolabeled PET tracers for iNOS has been limited¹² compared with the relatively rapid development of novel iNOS inhibitors as pharmaceuticals. In this paper, we describe the synthesis and screening of a series of position-6 substituted 2-amino-4-methylpyridine analogues as potential PET tracers for imaging iNOS, the radiosynthesis of [^{18}F]**9**, and the *in vivo* evaluation of [^{18}F]**9** in a mouse model of lipopolysaccharide (LPS)-induced iNOS activation.

Results and Discussion

Chemistry

The previously reported method was applied to synthesize the key intermediate **6** (Scheme 1).¹⁰ Compound **6** reacted with acetaldehyde to afford **7** in high yield (Scheme 2). Compound **7** was converted to **8** using diethylaminosulfur trifluoride (DAST) or perfluorobutane sulfonyl fluoride (PBSF) as the fluorinating agents. Compound **10** was obtained as a by-product in both cases and was formed as the major product when PBSF was used as the fluorinating agent. These results indicate the facile elimination to form a conjugated double bond adjacent to the pyridine ring. The conversion of the OH in **7** to Br using PPh₃ and CBr₄ failed to give the expected product (data not shown). Compounds **12** and **14** were synthesized from **7** via O-alkylation using CH₃I and BrCH₂CH₂F, respectively in the presence of CaH₂ (Scheme 2). The pyrrole protecting group in all the 2-amino pyridine analogues was removed by refluxing in an aqueous ethanol solution of hydroxylamine hydrochloride as previous reported.¹¹ Although no details were given in the reference, we found that a 2:1 mixture of ethanol and water (containing 4 M NH₂OH·HCl) at 110 °C afforded good results. The nucleophilic substitutions of BrCH₂CH₂F, BrCH₂CH₂CH₂F, and (CH₃)₃SiCl by **6** afforded **17**, **19**, and **21**, respectively in high yields (Scheme 3). Among the compounds synthesized, **9**, **13**, **15**, **16**, **27**, **30**, and **33** are racemic mixtures which were used without chiral resolution in the following studies.

The Peterson olefination reaction¹³ using α -trimethylsilyl carbanion **22** and the corresponding ketones was used to synthesize **23**, **25**, **28**, and **31**, respectively (Scheme 4). Compound **22** was

synthesized by reacting **21** with one equivalent of *n*-butyl lithium in good yield, which was evidenced by the good yield of **23** following the reaction with acetone. *E/Z* isomers were observed in these reactions and the isomers were reduced either by ammonium formate/ethanol in the presence of palladium on carbon (**25** and **28**) or by magnesium in ethanol (**31**). The former method was unsuccessful for the synthesis of **32**, most likely due to the poisoning of the palladium catalyst by the sulfur atom in **31**.

The synthesis of precursor **38** for the nucleophilic labeling of [¹⁸F]**9** is shown in Scheme 5. The hydroxyl group in the 2-hydroxypropyl group had to be protected as the corresponding acetate ester during the reaction with di-*tert*-butyldicarbonate (Boc₂O). Without protection of the -OH, **37** was only a minor product with the major product as the corresponding *t*-butylcarbonate and other by-products (data not shown). The acetylation to make **34** from **7** using acetyl chloride was slow and the yield was only 39%, probably due to steric hindrance from the secondary alcohol and the pyridine ring. A more efficient method of making **34** involved treating **6** with acetaldehyde followed by treatment with ethyl acetate to give **34** in an overall yield of 43%.

The synthesis of the mesylate and tosylate precursors required for the radiosynthesis of [¹⁸F]**18** failed to afford the desired products. It was found that the mesylate precursor formed initially but converted quickly even at room temperature to a cyclic 1-substituted pyridinium via an internal nucleophilic attack of the mesylate group by the pyridine nitrogen atom, and this cyclized product was confirmed by mass spectrometry, ¹H NMR and elemental analysis (data not shown). Therefore, attempts to radiolabel **18** were not successful and our efforts focused on radiolabeling **9** with ¹⁸F.

Radiosynthesis of [¹⁸F]**9**

[¹⁸F]**9** was synthesized via a nucleophilic substitution of the mesylate precursor **38** with [¹⁸F] fluoride, followed by deprotection with 1N HCl (Scheme 6). The incorporation of [¹⁸F] fluoride was only 10-20% at optimized conditions; however, after reversed phase HPLC purification, [¹⁸F]**9** was obtained in high chemical and radiochemical purity. The specific activity was >1,000 mCi/μmol at the end of synthesis. The total synthesis and purification time was 120 min and the isolated yield was up to 10% (decay corrected). The low incorporation of [¹⁸F] fluoride should be due to the slow rate of nucleophilic substitution on the secondary carbon, and the base-catalyzed elimination to form the corresponding nonreactive olefin. The radiolabeling using acetonitrile as the solvent gave a higher yield than that in DMF; use of the corresponding tosylate and triflate precursors gave a much lower yield or no incorporation of ¹⁸F at all.

In vitro enzyme assays

The inhibition potency for recombinant iNOS, eNOS and nNOS was determined using commercial Nitric Oxide Synthase Screening Kit (GE Healthcare Biosciences Corp., Piscataway, NJ) following the manufacturer's protocol with minor modifications. The assay was validated using standard NOS inhibitors. Only the most potent iNOS inhibitors were further evaluated for eNOS and nNOS potency to determine the selectivity between iNOS and eNOS or nNOS.

As shown in Table 1, the most potent compound for iNOS was **18**, with approximately 30-fold selectivity against eNOS and 10-fold against nNOS; **9** and **20** showed less potency for iNOS and less selectivity against eNOS and nNOS, but were comparable to the previously reported compound **2**, which had a potency of IC₅₀ = 193 nM for iNOS in our assay (The reported IC₅₀ of **2** is 28 nM¹⁰). We cannot determine the reasons for the difference between our value and the reported data, but slow time-dependent inhibition has been frequently reported.^{8b, 11, 14,}

¹⁵The IC₅₀ value may be influenced by the incubation time, longer incubation time may deliver more potent IC₅₀ values. Additionally, the measured inhibition potency may depend on the concentrations of NADPH and L-arginine.¹⁵ Nevertheless, the assay was validated by standard iNOS inhibitors (Table 1), and **9**, **18** and **20** were identified as potential PET tracers for imaging iNOS according to our assay results.

It has been reported previously that the 6-position of the pyridine ring has the greatest amount of bulk tolerance with respect to potency for inhibiting iNOS. Therefore, several 6-substituted analogs were synthesized in order to further investigate this structure-activity relationship. When the 2'-methyl group in lead compound **2** was replaced with a fluorine atom (i.e., **9**) the potency for iNOS remained the same. Introduction of a double bond to **2** to give an alkene analog, **24**, resulted in a diminished potency for iNOS. Removal of the *cis* methyl from **24** (i.e., **11**) regained the potency for iNOS (IC₅₀ = 282 nM); this change in potency for iNOS from **24** and **11** implies that steric demand at the 6-position is high. The change from the methyl in **2** or fluorine in **9** to the hydroxy group in **16** resulted in a large reduction in potency for iNOS, suggesting an adverse electronic substituent effect in this position. The corresponding methoxy (i.e., **13**) and 2-fluoroethoxy (i.e., **15**) analogs were inactive. Compound **18**, an isomer of **9** with the fluorine at the terminal position, had enhanced potency and selectivity for iNOS; however, extension of the alkyl chain in **18** by one methylene group (i.e., **20**) resulted in a reduction of potency for iNOS. Addition of a methyl group in the 2'-position of **20** to give **30** resulted in a further decrease in potency for iNOS. The corresponding MeO or MeS analogs, **27** and **33**, were inactive in the iNOS assay. In summary, there appear to be significant steric and electronic constraints for substituents at the 6-position of the pyridine ring with respect to potency for inhibiting iNOS.

***In vitro* stability and *in vivo* metabolism studies**

An *in vitro* stability study was carried out using heparinized rat blood taken from an adult male Sprague-Dawley rat. [¹⁸F]**9** was relatively stable in the whole blood for the duration of the experiment (2 h) at 37 °C. At 1 h, ~80% of the activity recovered from lysed whole blood was observed as [¹⁸F]**9**, and at 2 h, ~75% of the recovered activity was still the parent compound. These data suggest that the blood is not a major site for compound degradation, which is in contrast to the previously reported ¹⁸F and ¹¹C labeled isothioureia analogues.^{12a}

The *in vivo* metabolic stability of [¹⁸F]**9** was evaluated in plasma samples obtained from an adult male Sprague-Dawley rat at 5 and 30 min post-injection. The supernatant extracts were analyzed by silica gel radio-TLC and reversed phase HPLC. After 30 min, the percent parent compound was only 20.2%. Additionally, within 5 min post-injection only 40.3% of the activity in the blood was [¹⁸F]**9**, which was confirmed by HPLC co-elution with non-radioactive **9**. According to the HPLC analysis, the major metabolite, constituting 50% of the activity in blood at 5 min post-injection, was very polar but was not free [¹⁸F]fluoride. This observation is also consistent with the low bone uptake reported below in the biodistribution studies (Table 2). Since [¹⁸F]**9** demonstrated reasonable *in vitro* stability in whole blood, the metabolite observed *in vivo* at 5 min in blood must be due to metabolism in peripheral organs.

***In vivo* biodistribution study**

The biodistribution studies were performed in mature male C57BL/6 mice: one group was treated with bacterial lipopolysaccharide (LPS) (10 mg/kg, i.v.) to induce iNOS expression and one group without LPS-treatment as control. LPS has been well documented to induce iNOS mRNA and protein expression in both rats and mice,¹⁶ and administration of LPS resulted in an elevated iNOS expression at 6-7 h post-LPS-treatment. The iNOS distribution in organs was reported recently in male BALB/c mice.^{16c} It has been demonstrated in that report that iNOS mRNA and protein expression 6 h after LPS stimulation is observed in many organs,

including lungs, heart, liver, spleen, gut, and kidneys. Among them, the highest iNOS expression was in the lungs, with moderate expression in the spleen and kidneys, and the lowest in the heart, gut, and liver.^{16c} Therefore, this endotoxin (LPS) lung injury mouse model was used to assess the efficiency of [¹⁸F]9 as an iNOS radiotracer.

The results of *in vivo* biodistribution studies in the normal and LPS-treated mice are shown in Table 2 and Figure 1. The highest uptake in both groups was observed in the liver and kidneys, which are likely to be the major metabolic and/or excretory sites for the tracer. Excluding the potential metabolic sites, the highest uptake was observed in the lungs and blood, followed by muscle, heart, and brain in both groups. The low bone uptake suggested that [¹⁸F]9 had a high degree of stability towards defluorination, considering the facile elimination to form a conjugated double bond at this position. Compared to the control group, the LPS-treated mice had a ~30% increase in tracer uptake in most of the organs at 1 h. In the organ expected to have the highest iNOS expression, the lungs, the increase in injected dose/gram (ID/g) was even more pronounced, 30% at 5 min, 60% at 30 min and 130% at 1 h. Because systemic LPS-induced acute lung injury results in pulmonary edema, the difference in total lung uptake between control and treated animals (i.e., %I.D.) is more dramatic than the %ID/g in the lung (Figure 1). The overall higher uptake in tissues of the LPS-treated mice compared to the controls is consistent with the previously reported systemic iNOS response with LPS treatment.^{16c} From 30 min to 1 h, the uptake in the LPS-treated mice washed out at a slower rate than that of the control mice, which again can be attributed to the specific binding of [¹⁸F]9 to iNOS. Based on the *in vivo* metabolic stability study in the blood of normal rat (Table 2), there should be little circulating [¹⁸F]9 left at 2 h post-injection. At 2 h post-injection, all the activity was washed out to the same low level and the uptake at 2 h post-injection should be due to the non-specific uptake of the metabolites. In previously reported biodistribution studies in rats injected with less potent and less selective ¹⁸F and ¹¹C labeled isothioureia analogues, about 30% higher uptake of ¹⁸F labeled analog was observed in lungs, blood, liver, kidneys, and heart of LPS-treated rats than that of normal rats at 10 min post-injection. However, the difference in uptake between the two groups the differences became insignificant at 30 min post-injection, possibly due to the rapid metabolism of these radiotracers. The more stable ¹¹C labeled analog showed 40% higher uptake at 30 min post-injection in the lungs of the LPS-treated rats than that of the control.^{12a} Compared to the previously described ¹⁸F labeled isothioureia analogue, [¹⁸F]9, with prolonged retention in the LPS-treated mice, is a suitable PET tracer for iNOS.

A standard Western blot was performed to compare the iNOS induction in lungs upon LPS stimulation versus untreated controls and the results are shown in Figure 2. Protein for the Western blot was obtained from the lungs harvested from treated and untreated animals in the biodistribution study. The first lane is the purified iNOS protein as a positive control. Protein from two control lungs and six LPS-treated lungs were evaluated. As indicated in Figure 2, neither of the control samples demonstrated iNOS expression whereas the LPS-treated samples all showed some degree of iNOS induction due to the response toward LPS stimulation. This result is consistent with the higher tracer uptake in the lungs of the LPS-treated mice in the biodistribution studies, suggesting iNOS-specific uptake of [¹⁸F]9.

Blocking study

In order to further demonstrate that the increased uptake in the LPS-treated mice was due to specific binding of [¹⁸F]9 to iNOS, blocking studies were carried out. First, the non-selective NOS inhibitor 2-amino-4-methylpyridine (**1**) (10 mg/kg, i.v.) failed to block the increased uptake in the LPS-treated mice (data not shown). A failure to block tracer uptake using non-selective NOS inhibitors S-methyl or S-ethyl isothioureia has been reported previously;^{12a} the failure was contributed to the blood pressure change caused by the blocking agents in the animal, which may alter the tracer uptake function. 2-amino-4-methylpyridine (**1**) elevates

blood pressure^{9a,10,17} and blocking of eNOS expression may also reduce the blood flow.¹⁸ Therefore, a highly selectively iNOS inhibitor is preferred in order to avoid the side-effects from non-selective inhibitors. *N*-(3-(aminomethyl)benzyl)acetamidine (1400W) is a slow, tight binding, and highly selective inhibitor of iNOS *in vitro* and *in vivo*,^{8b} and has been used commonly as an iNOS inhibitor in many reported studies. However, due to its high toxicity,¹⁹ only 5 mg/kg of 1400W was injected intravenously immediately before the injection of [¹⁸F]**9**. The results are shown in Figure 3. At 1 h post injection of [¹⁸F]**9**, 32% of the tracer uptake in the lungs and blood of the LPS-treated mice was blocked by 1400W (Figure 3). This reduced uptake in the lungs of the LPS-treated mice should be due to the specific blocking of iNOS by 1400W, and is consistent with that the uptake of [¹⁸F]**9** in the LPS-treated mice is iNOS specific.

MicroPET study

A microPET imaging study using [¹⁸F]**9** was carried out on an intratracheally LPS-treated mouse and a normal mouse as control. The microPET images (0-60 min dynamic scan) are shown in Figure 4. As shown in the microPET images (Figure 4), accumulation of [¹⁸F]**9** was observed in the target organ, the lungs, of the LPS-treated mouse, whereas no such accumulation was observed in the lungs of normal mouse. The difference in the tracer uptake in the lungs of the LPS-treated and control mice is consistent with iNOS expression induced by LPS treatment and is similar to the results of biodistribution study.

Conclusion

We have identified 6-(2-fluoropropyl)-4-methylpyridin-2-amine (**9**), 6-(3-fluoropropyl)-4-methylpyridin-2-amine (**18**), and 6-(4-fluorobutyl)-4-methylpyridin-2-amine (**20**) as iNOS inhibitors with the greatest potential to serve as PET radiotracers. [¹⁸F]**9** was synthesized in modest yield (~10%), but with high chemical and radiochemical purities. In the biodistribution study of a mouse model of LPS-induced iNOS activation, higher uptake of [¹⁸F]**9** was observed in the lungs of the LPS-treated mice than those in the control mice. The higher uptake in the lungs of the LPS-treated animals correlated well with iNOS expression, which was confirmed by Western blot analysis of the lung samples from control and LPS-treated mice. The increased uptake in the lungs of the LPS-treated mice at 60 min post injection of [¹⁸F]**9** was reduced by injection of the highly selective iNOS inhibitor, 1400W. The blocking study suggests that the higher uptake of [¹⁸F]**9** in the lungs of the LPS-treated mice is due to specific binding of [¹⁸F]**9** to [iNOS]. MicroPET study of the LPS-treated mouse using [¹⁸F]**9** demonstrated an accumulation of [¹⁸F]**9** in the lungs of the LPS-treated mice, in sharp contrast to those of the control mouse. In conclusion, [¹⁸F]6-(2-Fluoropropyl)-4-methylpyridin-2-amine ([¹⁸F]**9**) is a potential radiotracer for PET imaging of iNOS expression.

Experimental Section

General methods and materials

All chemicals were obtained from standard commercial sources and used without further purification. All reactions were carried out by standard air-free and moisture-free techniques under an inert argon atmosphere with dry solvents unless otherwise stated. Flash column chromatography was conducted using Scientific Adsorbents, Inc. silica gel, 60A, "40 Micron Flash" (32-63 μ m). Melting points were uncorrected. Routine ¹H NMR spectra were recorded at 300 MHz. All chemical shifts were reported as a part per million (ppm) downfield from tetramethylsilane (TMS) or when chloroform-d was used as solvent and the solvent peak at δ 7.25 ppm was used as an internal standard. All coupling constants (*J*) are given in Hz. Splitting patterns are typically described as follows: s, singlet; d, doublet; t, triplet; m, multiplet. ¹⁹F NMR spectra were recorded at 282.2 MHz, and chemical shifts are reported as Hz upfield from

an external CFCl_3 standard. ESI/MS was performed on a Waters ZQ 4000 single quadrupole mass spectrometer equipped with an electrospray ionization (ESI) LC-MS interface. High performance liquid chromatography (HPLC) was performed with an ultraviolet detector operating at 251 nm and a well-scintillation NaI (Tl) detector and associated electronics for radioactivity detection. Alltech Platinum EPS C18 250 \times 10 mm semi-preparative column and Alltech Platinum EPS C18 250 \times 4.6 mm analytical column were used for preparation and analysis respectively. 4-Methoxybutan-2-one was synthesized according to literature.²⁰ The purities of final compounds are $\geq 95\%$, which were confirmed by examination of elemental analysis results or by reversed phase HPLC (for compound **13**, **15**, **18**, **24**, and **27**).

H_2 ^{18}O was purchased from Rotem Industries (Israel). [^{18}F]Fluoride was produced in Washington University by the $^{18}\text{O}(\text{p},\text{n})^{18}\text{F}$ reaction through proton irradiation of enriched (95%) ^{18}O water using RDS111 cyclotron. Materials were heated using a custom-designed microwave cavity, model 420BX (Micro-Now Instruments, Skokie, IL). Screw-cap test tubes used for microwave heating were purchased from Fisher Scientific (Pyrex No. 9825). HLB Sep-Pak cartridges were purchased from Waters Corporation. For the TLC analyses, EM Science Silica Gel 60 F₂₅₄ TLC plates were purchased from Fisher Scientific (Pittsburgh, PA). Radio-TLC was accomplished using a Bioscan 200 imaging scanner (Bioscan, Inc., Washington, DC). Radioactivity was counted with a Beckman Gamma 6000 counter containing a NaI crystal (Beckman Instruments, Inc., Irvine, CA).

Typical procedure for the synthesis of **6**

Into a solution of **5** (2.0 g, 10 mmol) in dry Et_2O (20 mL) at -20 °C was added dropwise *n*-BuLi (1.6 M in Hexane, 6.9 mL, 10 mmol) within 5 min, then the reaction mixture was stirred at -20 to -10 °C for 1 h to complete the reaction. Orange solids precipitated gradually during the experiment, and the reaction mixture of **6** was used directly for further reactions.

1-(6-(2,5-Dimethyl-1*H*-pyrrol-1-yl)-4-methylpyridin-2-yl)propan-2-ol (**7**)

Into an Et_2O solution of **6** at -78 °C, which was made from **5** (5.6 g, 28.0 mmol), *n*-BuLi (1.6 M in Hexane, 19.5 mL, 31.2 mmol) in Et_2O (30 mL), was added CH_3CHO (2 mL, 35.6 mmol) via a syringe. The reaction mixture was allowed to warm up to room temperature and stirring was continued for 10 min. Then, the reaction mixture was treated with H_2O (100 mL), and extracted with ethyl acetate (3×50 mL). The organic solution was washed with brine (2×30 mL), dried over Na_2SO_4 and the solvent was evaporated under reduced pressure. The crude product was purified with silica gel chromatograph using 1:4 ethyl acetate/hexanes to afford **7** (5.6 g) in 80 % yield as colorless liquid. ^1H NMR (CD_3Cl , 300 MHz) δ 6.97 (s, 1H), 6.89 (s, 1H), 5.87 (s, 2H), 4.51 (s, br, 1H), 4.23 (m, 1H), 2.94-2.80 (m, 2H), 2.39 (s, 3H), 2.12 (s, 6H), 1.25 (d, 3H, $J = 6.3$ Hz).

2-(2,5-Dimethyl-1*H*-pyrrol-1-yl)-6-(2-fluoropropyl)-4-methylpyridine (**8**)

Using diethylaminosulfur trifluoride (DAST) as fluorinating agent—Into a solution of **7** (0.5 g, 2.05 mmol) in CH_2Cl_2 (5 mL) at 0 °C was added DAST (0.4 mL, 3.05 mmol) dropwise. The reaction mixture became brown in color, and the starting material was consumed within 30 min. Saturated NaHCO_3 solution (10 mL) was added to quench the reaction, and the aqueous solution was extracted with ethyl acetate (2×30 mL). The organic layers was washed with brine (2×30 mL) and dried over Na_2SO_4 . Solvents were evaporated under reduced pressure and the crude product was purified with silica gel chromatograph using 1:10 ethyl acetate/hexanes to afford **8** (0.13 g) in 26 % yield as colorless liquid. ^1H NMR (CD_3Cl , 300 MHz) δ 7.08 (s, 1H), 6.93 (s, 1H), 5.91 (s, 2H), 5.05-5.60 (m, 1H), 3.20 (m, 2H), 2.43 (s, 3H), 2.15 (s, 6H), 1.43 (dd, 3H, $J = 23.4, 6.3$ Hz); ESI/MS m/z 247.06 [$\text{M}+\text{H}^+$].

Using perfluorobutane sulfonyl fluoride (PBSF) as fluorinating agent—Into a solution of **7** (0.5 g, 2.05 mmol) in CH₃CN (5 mL) were added PBSF (0.74 mL, 4.1 mmol), Et₃N (1.73 mL, 12.4 mmol) and (NEt₃)(HF)₃ (0.67 mL, 4.11 mmol). The reaction mixture was stirred quickly and became homogenous after 40 min. The reaction was complete in 2.5 h according to TLC analysis, and the solvent was evaporated under reduced pressure. Silica gel chromatograph purification of the residue using 1:10 ethyl acetate/hexanes afforded **8** (0.13 g) in 26 % yield as colorless liquid.

6-(2-Fluoropropyl)-4-methylpyridin-2-amine (9): Typical procedure for the deprotection

Into a 50 mL round-bottom flask equipped with a magnetic stirring bar and a condenser were added **8** (1.10 g, 4.1 mmol) and NH₂OH·HCl (10 g, 144 mmol), followed by ethanol (25 mL) and water (12.5 mL). The reaction mixture was stirred at reflux and the reaction was monitored by TLC. Upon the completion of the reaction in about 3 h, the reaction mixture was treated with saturated Na₂CO₃ solution (10 mL) and extracted with CH₂Cl₂ (3 × 20 mL). The combined organic layers was washed with brine (2 × 20 mL) and dried over Na₂SO₄. After removal of volatiles under reduced pressure, the crude product was purified with silica gel chromatograph using ethyl acetate to afford **9** (0.61 g) in 81 % yield as light yellow solid (mp. 51.0-52.5 °C; oxalate 154.0-155.9 °C). The oxalate was precipitated using 1:1 of **9** and oxalic acid in ethyl acetate to afford the salt as a white solid. ¹H NMR (CD₃Cl, 300 MHz) δ 6.40 (s, 1H), 6.18 (s, 1H), 5.20-4.90 (m, 1H), 4.37 (s, br, 2H), 3.00-2.70 (m, 2H), 2.19 (s, 3H), 1.37 (dd, 3H, *J* = 24.0, 6.3 Hz).

(E)-2-(2,5-Dimethyl-1H-pyrrol-1-yl)-4-methyl-6-(prop-1-enyl)pyridine (10)

10 was obtained as a by-product during the synthesis of **9** using PBSF as fluorinating agent in 49 % yield as colorless liquid. ¹H NMR (CD₃Cl, 300 MHz) δ 7.00 (s, 1H), 6.83 (s, 1H), 6.85-6.78 (m, 1H), 6.51-6.44 (s, 1H), 5.88 (s, 2H), 2.38 (s, 3H), 2.15 (s, 6H), 1.92 (d, 3H, *J* = 6.9 Hz).

(E)-4-Methyl-6-(prop-1-enyl)pyridin-2-amine (11)

11 was synthesized from **10** using the standard deprotection procedure in 53 % yield as a solid (mp. 66.4-67.0 °C; oxalate 137.5-138.7 °C). ¹H NMR (CD₃Cl, 300 MHz) δ 6.67-6.56 (m, 1H), 6.40 (s, 1H), 6.28 (d, 1H, *J* = 15.3 Hz), 6.14 (s, 1H), 4.42 (s, br, 2H), 2.17 (s, 3H), 1.86 (d, 3H, *J* = Hz).

2-(2,5-Dimethyl-1H-pyrrol-1-yl)-6-(2-methoxypropyl)-4-methylpyridine (12)

Into a solution of **7** (0.9 g, 3.68 mmol) in freshly distilled THF (20 mL) was added 60% NaH in mineral oil (0.3 g, 12.6 mmol). After 5 min, MeI (0.5 mL, 8.03 mmol) was added, and the reaction mixture was stirred at room temperature for 5 h. The mixture was then quenched with an aqueous 1 N HCl solution, followed by neutralization with saturated solution of aqueous Na₂CO₃. The product was extracted with ethyl acetate (3 × 20 mL) and the combined organic layers was washed with brine (30 mL) and dried over MgSO₄. After evaporation of solvents under reduced pressure, silica gel chromatograph purification of the residue using 1:4 ethyl acetate/hexanes afforded **12** (0.89 g) in 94% yield as a light yellow liquid. ¹H NMR (CD₃Cl, 300 MHz) δ 7.01 (s, 1H), 6.86 (s, 1H), 5.87 (s, 2H), 3.84 (m, 1H), 3.30 (s, 3H), 3.05-2.70 (m, 2H), 2.39 (s, 3H), 2.11 (s, 6H), 1.17 (d, 3H, *J* = 6.0 Hz).

6-(2-Methoxypropyl)-4-methylpyridin-2-amine (13)

13 was synthesized from **12** using the standard deprotection method. The corresponding oxalate was precipitated using 1:1 of **13** and oxalic acid in ethyl acetate to afford the salt as a white solid (mp. oxalate 123-125 °C). ¹H NMR (CD₃Cl, 300 MHz) δ 6.35 (s, 1H), 6.13 (s, 1H), 4.49 (s, br, 2H), 3.71 (m, 1H), 3.30 (s, 3H), 2.89-2.49 (m, 2H), 2.16 (s, 3H), 1.12 (d, 3H, *J* = 6 Hz).

2-(2,5-Dimethyl-1H-pyrrol-1-yl)-6-(2-(2-fluoroethoxy)propyl)-4-methylpyridine (14)

Into a solution of **7** (1.0 g, 4.1 mmol) in freshly distilled THF (20 mL) were added 60 % NaH in mineral oil (0.35 g, 8.8 mmol) and 1-bromo-2-fluoroethane (1.0 mL, 8 mmol). The reaction mixture was stirred at room temperature for 6 h, then at 60 °C overnight. The reaction mixture was filtered and the organic solution was washed with 1 N HCl solution, saturated Na₂CO₃, and brine and then dried over Na₂SO₄. Solvent was evaporated under reduced pressure and the residue was purified by silica gel chromatograph using 1:8 ethyl acetate/hexanes to afford **14** (0.37 g) in 31 % yield as colorless liquid. ¹H NMR (CD₃Cl, 300 MHz) δ 7.04 (s, 1H), 6.86 (s, 1H), 5.87 (s, 2H), 4.54- 4.35 (m, 2H), 3.97 (m, 1H), 3.79-3.53 (m, 2H), 3.09-2.81 (m, 2H), 2.38 (s, 3H), 2.10 (s, 6H), 1.20 (d, 3H, *J* = 6.3 Hz).

6-(2-(2-Fluoroethoxy)propyl)-4-methylpyridin-2-amine (15)

15 was synthesized from **14** using the standard deprotection procedure in 81% yield as solid (mp. 60.2-63.0 °C; oxalate 163- 164 °C). ¹H NMR (CD₃Cl, 300 MHz) δ 6.40 (s, 1H), 6.16 (s, 1H), 4.56-4.37 (m, 2H), 4.35 (s, br, 2H), 3.88 (m, 1H), 3.67-3.53 (m, 2H), 2.92-2.55 (m, 2H), 2.18 (s, 3H), 1.18 (d, 3H, *J* = 6.3 Hz).

1-(6-Amino-4-methylpyridin-2-yl)propan-2-ol (16)

16 was synthesized from **7** using the standard deprotection procedure in 66 % yield as a light yellow solid (mp. 95-96 °C). ¹H NMR (CD₃Cl, 300 MHz) δ 6.31 (s, 1H), 6.18 (s, 1H), 4.30 (s, br, 1H), 4.12 (m, 1H), 2.62 (m, 2H), 2.19 (s, 3H), 1.23 (d, 3H, *J* = 6.0 Hz).

2-(2,5-Dimethyl-1H-pyrrol-1-yl)-6-(3-fluoropropyl)-4-methylpyridine (17)

Into an Et₂O solution of **5** at -78 °C, which was made from **3** (2.0 g, 10 mmol), *n*-BuLi (1.6 M in Hexane, 8.0 ml, 12.8 mmol) in Et₂O (20 ml), was added BrCH₂CH₂F (2.0 g, 15.7 mmol) via a syringe. The reaction mixture was allowed to warm up to room temperature and continued to stir for 30 min. Then, the reaction mixture was treated with saturated Na₂CO₃ solution and then brine. The organic solution was dried over Na₂SO₄ and the solvent was evaporated under reduced pressure. The crude product was purified with silica gel chromatograph using 1:8 ethyl acetate/hexanes to afford **29** (1.6 g) in 61 % yield as colorless liquid. ¹H NMR (CD₃Cl, 300 MHz) δ 7.04 (s, 1H), 6.91 (s, 1H), 5.92 (s, 2H), 4.53 (dt, 2H, *J* = 6.0, 47.4 Hz), 2.95 (t, 2H, *J* = 7.5 Hz), 2.44 (s, 3H), 2.3-2.1 (m, 2H), 2.16 (s, 6H); ¹⁹F NMR (CD₃Cl, 282.2 MHz) δ: -42.9.

6-(3-Fluoropropyl)-4-methylpyridin-2-amine (18).

18 was synthesized from **17** using the standard deprotection procedure in 55 % yield as light yellow solid (mp. oxalate 112 °C decomposition). ¹H NMR (CD₃Cl, 300 MHz) δ 6.35 (s, 1H), 6.14 (s, 1H), 4.45 (dt, 2H, *J* = 6.0, 47.1 Hz), 4.37 (s, br, 2H), 2.66 (t, 2H, *J* = 7.6 Hz), 2.18 (s, 3H), 2.20-2.00 (m, 2H); ¹⁹F NMR (CD₃Cl, 282.2 MHz) δ -42.6.

2-(2,5-Dimethyl-1H-pyrrol-1-yl)-6-(4-fluorobutyl)-4-methylpyridine (19)

Into an Et₂O solution of **6** at -78 °C, which was made from **5** (3.0 g, 15 mmol), *n*-BuLi (1.6 M in Hexane, 11.0 ml, 17.6 mmol) in Et₂O (30 ml), was added BrCH₂CH₂CH₂F (2.1 g, 15.0 mmol) via a syringe. The reaction mixture was allowed to warm up to room temperature and continued to stir for 30 min. The reaction mixture was then treated with saturated Na₂CO₃ solution and brine. The organic was dried over Na₂SO₄ and the solvent was evaporated under reduced pressure. The crude product was purified with silica gel chromatograph using 1: 10 ethyl acetate/hexanes to afford **19** (2.5 g) in 63 % yield as colorless liquid. ¹H NMR (CD₃Cl, 300 MHz) δ 6.98 (s, 1H), 6.85 (s, 1H), 5.87 (s, 2H), 4.47 (dt, 2H, *J* = 6.0, 47.1 Hz), 2.82 (t, 2H, *J* = 7.5 Hz), 2.39 (s, 3H), 2.11 (s, 6H), 1.9-1.7 (m, 4H); ¹⁹F NMR (CD₃Cl, 282.2 MHz) δ - 41.7.

6-(4-Fluorobutyl)-4-methylpyridin-2-amine (20)

20 was synthesized from **19** using the standard deprotection procedure in 57 % yield as light yellow solid (mp. Oxalate 133.0-135.0 °C). ¹HMR (CD₃Cl, 300 MHz) δ 6.33 (s, 1H), 6.14 (s, 1H), 4.44 (dt, 2H, *J* = 6.0, 47.4 Hz), 4.38 (s, br, 2H), 2.58 (t, 2H, *J* = 7.4 Hz), 2.18 (s, 3H), 1.8-1.65 (m, 4H). ¹⁹F NMR (CD₃Cl, 282.2 MHz) δ: - 41.5.

2-(2,5-Dimethyl-1 *H*-pyrrol-1-yl)-4-methyl-6-((trimethylsilyl)methyl)pyridine (21)

Into an Et₂O solution of **6** at -78 °C, which was made from **5** (5.78 g, 28.9 mmol), *n*-BuLi (1.6 M in Hexane, 21.6 mL, 34.6 mmol) in Et₂O (50 mL), was added Me₃SiCl (4.4 mL, 34.6 mmol) via a syringe. The reaction mixture was allowed to warm to room temperature and continued to stir for 30 min. Then, the reaction mixture was treated with saturated Na₂CO₃ solution and washed with brine. The organic solution was dried over Na₂SO₄ and the solvent was evaporated under reduced pressure. The crude product was purified with silica gel chromatograph using 1:4 ethyl acetate/hexanes to afford **21** (7.4 g) in 94 % yield as colorless liquid. ¹H NMR (CD₃Cl, 300 MHz) δ 6.79 (s, 1H), 6.72 (s, 1H), 5.84 (s, 2H), 2.35 (s, 2H), 2.07 (s, 6H), 0.03 (s, 9H); ESI/MS: *m/z* 273.2 (M+H⁺).

2-(2,5-Dimethyl-1 *H*-pyrrol-1-yl)-4-methyl-6-(2-methylprop-1-enyl)pyridine (23)

Into a solution of **21** (1.0 g, 3.67 mmol) in Et₂O (10 mL) at -20 °C was added dropwise *n*-butyl lithium (1.6 M in hexane, 2.75 mL, 4.4 mmol). The reaction solution turned brown in color and was stirred at -20 to -10 °C for 2 h to afford a solution of ((6-(2,5-dimethyl-1*H*-pyrrol-1-yl)-4-methylpyridin-2-yl)(trimethylsilyl)methyl)lithium (**22**). The solution was then cooled to -78 °C, and 2 ml acetone was added. The solution became clear in slightly yellow color, and it was allowed to warm up to room temperature during 20 min. The organic solution was acidified with 1 N HCl (6 mL), followed by washing with saturated Na₂CO₃ solution, brine, and dried over Na₂SO₄. Solvent was evaporated under reduced pressure and the crude product was purified with silica gel chromatograph using 1:15 ethyl acetate/hexanes to afford **23** (0.56 g) in 64 % yield as colorless liquid. ¹H NMR (CD₃Cl, 300 MHz) δ 6.97 (s, 1H), 6.79 (s, 1H), 6.28 (s, 1H), 5.86 (s, 2H), 2.38 (s, 3H), 2.13 (s, 6H), 2.12 (s, 3H), 1.94 (s, 3H); ESI/MS: *m/z* 241.2 (M+H⁺).

4-Methyl-6-(2-methylprop-1-enyl)pyridin-2-amine (24)

24 was synthesized from **23** using the standard deprotection procedure in 64 % yield as slightly yellow liquid (mp. oxalate 154-156 °C). ¹H NMR (CD₃Cl, 300 MHz) δ 6.38 (s, 1H), 6.13 (s, 1H), 6.12 (s, 1H), 4.37 (s, br, 2H), 2.17 (s, 3H), 1.99 (s, 3H), 1.87 (s, 3H).

(*E/Z*)-2-(2,5-Dimethyl-1 *H*-pyrrol-1-yl)-6-(4-methoxy-2-methylbut-1-enyl)-4-methylpyridine (25)

Into an Et₂O solution of **22** at -78 °C, which was made from **21** (1.0 g, 3.67 mmol), *n*-BuLi (1.6 M in Hexane, 2.75 mL, 4.4 mmol) in Et₂O (10 mL), was added 4-methoxybutan-2-one (0.45 g, 4.4 mmol). After the addition, the reaction mixture was allowed to warm up to room temperature during 30 min. The mixture was then acidified with 1 N HCl (6 mL), neutralized by saturated Na₂CO₃ solution and diluted with ethyl acetate (50 mL). The organic solution was washed with brine and dried over Na₂SO₄. Solvent was evaporated under reduced pressure and the crude product was purified with silica gel chromatograph using 1:15 and 1:8 ethyl acetate/hexanes to afford *E* and *Z* isomers of **23** (0.25 g and 0.22 g) in 45 % total yield as colorless liquid. ¹H NMR (CD₃Cl, 300 MHz) δ 7.01 (s, 1H), 6.81 (s, 1H), 6.35 (s, 1H), 5.85 (s, 2H), 3.55 (t, 2H, *J* = 7.2 Hz), 3.25 (s, 3H), 2.90 (t, 2H, *J* = 7.2 Hz), 2.38 (s, 3H), 2.11 (s, 6H), 1.97 (s, 3H) and δ 7.00 (s, 1H), 6.80 (s, 1H), 6.33 (s, 1H), 5.87 (s, 2H), 3.58 (t, 2H, *J* = 6.6 Hz), 3.37 (s, 3H), 2.48 (t, 2H, *J* = 6.90 Hz), 2.38 (s, 3H), 2.16 (s, 3H), 2.13 (s, 6H).

2-(2,5-Dimethyl-1H-pyrrol-1-yl)-6-(4-methoxy-2-methylbutyl)-4-methylpyridine (26)

Into a 100 mL round-bottom flask equipped with a magnetic stirring bar were loaded the isomeric mixture of **25** (0.47 g, 1.7 mmol) and absolute EtOH (20 mL), followed by 10% Pd/C (0.25 g). The reaction mixture was stirred in an 80° C oil bath, and the reaction was completed in 1 h according to TLC analysis. Solids were removed by filtration and solvent was evaporated under reduced pressure. The residue was dissolved in ethyl acetate and the organic solution was treated with saturated Na₂CO₃ solution (10 mL) and washed with brine, dried over MgSO₄. Solvent was evaporated under reduced pressure and the crude product was purified with silica gel chromatograph using 1:10 and 1:4 ethyl acetate/hexanes to afford **26** (0.38 g) in 81 % yield as colorless liquid. ¹H NMR (CD₃Cl, 300 MHz) δ 6.94 (s, 1H), 6.83 (s, 1H), 5.86 (s, 2H), 3.41 (m, 2H), 3.30 (s, 3H), 2.82-2.55 (m, 2H), 2.37 (s, 3H), 2.15 (m, 1H), 2.10 (s, 6H), 1.69-1.44 (m, 2H), 0.90 (d, 3H, *J* = 6.60 Hz).

Synthesis of 6-(4-methoxy-2-methylbutyl)-4-methylpyridin-2-amine (27)

27 was synthesized from **26** using the standard deprotection procedure in 71 % yield as slightly yellow solid (mp. 48.0-50.0 °C). ¹H NMR (CD₃Cl, 300 MHz) δ 6.32 (s, 1H), 6.14 (s, 1H), 4.35 (s, br, 2H), 3.42 (m, 2H), 3.30 (s, 3H), 2.59-2.33 (m, 2H), 2.18 (s, 3H), 2.05 (m, 1H), 1.70-1.40 (m, 2H), 0.89 (d, 3H, *J* = 6.90 Hz).

(E/Z)-2-(2,5-Dimethyl-1H-pyrrol-1-yl)-6-(4-fluoro-2-methylbut-1-enyl)-4-methylpyridine (28)

28 was synthesized from **22** using the standard deprotection method in 50% yield as a colorless liquid. ¹H NMR (CD₃Cl, 300 MHz) δ 6.97 (s, 1H), 6.79 (s, 1H), 6.38 (s, 1H), 4.61 (dt, 2H, *J* = 6.0, 47.1 Hz), 2.60 (dt, 2H, *J* = 6.1, 24.0 Hz), 2.38 (s, 3H), 2.10 (s, 6H), 2.00 (s, 3H) and δ 7.01 (s, 1H), 6.82 (s, 1H), 6.36 (s, 1H), 4.63 (dt, 2H, *J* = 6.3, 47.1 Hz), 3.09 (dt, 2H, *J* = 6.1, 25.2 Hz), 2.39 (s, 3H), 2.18 (s, 3H), 2.13 (s, 6H).

2-(2,5-Dimethyl-1H-pyrrol-1-yl)-6-(4-fluoro-2-methylbutyl)-4-methylpyridine (29)

29 was synthesized from a mixture of **28** using ammonium formate in the presence of 10% Pd/C in 30% yield as colorless liquid. ¹H NMR (CD₃Cl, 300 MHz) δ 6.95 (s, 1H), 6.85 (s, 1H), 5.86 (s, 2H), 4.50 (dt, 2H, *J* = 6.0, 47.4 Hz), 2.83-2.59 (m, 2H), 2.38 (s, 3H), 2.28-2.18 (m, 1H), 2.06 (s, 6H), 1.87-1.48 (m, 2H), 0.93 (d, 3H, *J* = 6.9 Hz).

6-(4-Fluoro-2-methylbutyl)-4-methylpyridin-2-amine (30)

30 was synthesized from **29** using the standard deprotection procedure in 47% yield as light yellow solid (oxalate: mp. 136.6-137.1 °C). ¹H NMR (CD₃Cl, 300 MHz) δ 6.31 (s, 1H), 6.15 (s, 1H), 4.67 (s, br, 2H), 4.50 (dt, 2H, *J* = 6.3, 47.4 Hz), 2.61-2.37 (m, 2H), 2.19 (s, 3H), 2.15-2.05 (m, 1H), 1.90-1.45 (m, 2H), 0.93 (d, 3H, *J* = 6.3 Hz); ¹⁹F NMR (CD₃Cl, 282.2 MHz) δ: -41.1.

(E/Z)-2-(2,5-Dimethyl-1H-pyrrol-1-yl)-4-methyl-6-(2-methyl-4-(methylthio)but-1-enyl)pyridine (31)

Into an Et₂O solution of **22** at -78 °C, which was made from **21** (1.6 g, 5.87 mmol), *n*-BuLi (1.6 M in Hexane, 4.8 mL, 7.68 mmol) in Et₂O (25 mL), was added 4-(methylthio)butan-2-one (0.90 g, 7.61 mmol). The reaction mixture was allowed to warm to room temperature over 30 min. The reaction solution was then acidified with 1 N HCl (10 mL), followed by neutralization by saturated Na₂CO₃ solution. The mixture was diluted with ethyl acetate (50 mL), and the organic solution was washed with brine, and dried over Na₂SO₄. Solvent was evaporated under reduced pressure and the crude product was purified with silica gel chromatograph using 1:10 ethyl acetate/hexanes to afford *E/Z* isomer mixture of **31** (1.38 g) in 78 % yield as colorless liquid. ¹H NMR (CD₃Cl, 300 MHz) δ 6.94 (s, 1H), 6.80 (s, 1H),

6.28 (d, 1H, $J = 1.5$ Hz), 5.83 (s, 2H), 2.90 (m, 2H), 2.62 (m, 2H), 2.37 (s, 3H), 2.09 (s, 6H), 1.95 (d, 3H, $J = 1.5$ Hz), 1.87 (s, 3H) and δ 7.00 (s, 1H), 6.80 (s, 1H), 6.32 (d, 1H, $J = 1.2$ Hz), 5.86 (s, 2H), 2.70 (m, 2H), 2.48 (m, 2H), 2.38 (s, 3H), 2.14 (s, 3H), 2.14 (d, 3H, $J = 1.2$ Hz), 2.12 (s, 6H).

2-(2,5-Dimethyl-1H-pyrrol-1-yl)-4-methyl-6-(2-methyl-4-(methylthio)butyl)pyridine (32)

Into a solution of **31** (1.38 g, 4.6 mmol) in EtOH (30 mL) at 0 °C was added Mg turnings (1.25 g, 51 mmol). The reaction mixture was stirred at 0 °C for 1 h, and then at room temperature overnight. All Mg turnings were consumed. The reaction mixture was acidified with 1 N HCl, and then treated with saturated Na₂CO₃ solution, extracted with ethyl acetate (3 × 150 mL). The organic layers were combined and the solvent was evaporated under reduced pressure. The residue was purified with silica gel chromatograph using 1:10 ethyl acetate/hexanes to afford **32** (0.42 g) in 30% yield as colorless liquid. ¹H NMR (CD₃Cl, 300 MHz) δ 6.97 (s, 1H), 6.86 (s, 1H), 5.88 (s, 2H), 2.80-2.50 (m, 4H), 2.40 (s, 3H), 2.15 (m, 1H), 2.12 (s, 6H), 2.07 (s, 3H), 1.7-1.5 (m, 2H), 0.92 (d, 3H, $J = 6.90$ Hz).

4-Methyl-6-(2-methyl-4-(methylthio)butyl)pyridin-2-amine (33)

33 was synthesized from **32** using the standard deprotection procedure in 84% yield as a light yellow solid (oxalate, mp. 103.0-103.5 °C). ¹H NMR (CD₃Cl, 300 MHz) δ 6.32 (s, 1H), 6.15 (s, 1H), 4.62 (s, br, 2H), 2.62-2.34 (m, 4H), 2.20 (s, 3H), 2.08 (s, 3H), 2.04 (m, 1H), 1.75-1.42 (m, 2H), 0.90 (d, 3H, $J = 6.6$ Hz).

1-(6-(2,5-Dimethyl-1H-pyrrol-1-yl)-4-methylpyridin-2-yl)propan-2-yl acetate (34)

Method 1—Into a solution of **7** (1.1 g, 4.50 mmol) in CH₂Cl₂ (20 mL) were added triethyl amine (0.94 mL, 6.75 mmol) and acetyl chloride (0.48 mL, 6.79 mmol). A white solid was formed instantly and the reaction was stopped at 10 min by addition of methanol (1 mL). The reaction mixture was treated with saturated NaHCO₃ solution, and the product was extracted with CH₂Cl₂ (2 × 50 mL) and dried over Na₂SO₄. Solvent was removed under reduced pressure and the residue was purified by silica gel chromatograph using 1:4 ethyl acetate/hexanes to afford **34** (0.5 g) in 39% yield as colorless liquid. ¹H NMR (CD₃Cl, 300 MHz) δ 7.00 (s, 1H), 6.89 (s, 1H), 5.87 (s, 2H), 5.31 (m, 1H), 4.48 (s, br, 2H), 3.11-2.93 (m, 2H), 2.40 (s, 3H), 2.10 (s, 6H), 1.97 (s, 3H), 1.28 (d, 3H, $J = 6.0$ Hz).

Method 2—Into an Et₂O solution of **6** at -78 °C, which was made from **5** (8.1 g, 40.5 mmol), *n*-BuLi (1.6 M in Hexane, 27.8 mL, 44.5 mmol) in Et₂O (120 mL), was added CH₃CHO (2.5 mL, 44.5 mmol) via a syringe. The reaction mixture was allowed to warm to room temperature over 30 min. The reaction mixture was cooled down to -78 °C and ethyl acetate (10 mL) was added. The mixture was allowed to warm to room temperature and stirring continued for an additional 30 min. The reaction mixture was treated with H₂O (100 mL), and the products were extracted with ethyl acetate (100 mL). The organic solution was washed with brine and water, dried over Na₂SO₄ and the solvent was evaporated under reduced pressure. The crude product was purified with silica gel chromatograph using 1:6, 1:4, and 1:1 ethyl acetate/petroleum ether to afford **7** (3.9 g) and **34** (4.85 g) as colorless liquids.

1-(6-Amino-4-methylpyridin-2-yl)propan-2-yl acetate (35)

35 was synthesized from **34** using the standard deprotection procedure in 55% yield as a light yellow solid (mp. 83-85 °C). ¹H NMR (CD₃Cl, 300 MHz) δ 6.37 (s, 1H), 6.19 (s, 1H), 5.25 (m, 1H), 4.48 (s, br, 2H), 2.92-2.68 (m, 2H), 2.20 (s, 3H), 1.99 (s, 3H), 1.25 (d, 3H, $J = 6.0$ Hz).

1-(6-(*tert*-Butoxycarbonylamino)-4-methylpyridin-2-yl)propan-2-yl acetate (36)

A solution of **35** (0.5 g, 2.4 mmol) and di-*tert*-butyl dicarbonate (1.2 g, 5.5 mmol) in *t*-BuOH (15 mL) was stirred in a 65 °C oil bath for 66 h. Solvent was removed under reduced pressure and the residue was purified by silica gel chromatograph using 1:4 ethyl acetate/hexanes to afford **36** (0.5 g) in 68% yield as colorless liquid. ¹HMR (CD₃Cl, 300 MHz) δ 7.61 (s, 1H), 6.65 (s, 1H), 5.26 (m, 1H), 2.95-2.71 (m, 2H), 2.30 (s, 3H), 1.97 (s, 3H), 1.50 (s, 9H), 1.23 (d, 3H, *J* = 6.0 Hz).

***tert*-Butyl 6-(2-hydroxypropyl)-4-methylpyridin-2-ylcarbamate (37)**

Into a solution of **36** (0.9 g, 2.9 mmol) in methanol (15 mL) was added a solution of K₂CO₃ (0.8 g, 5.7 mmol) in water (6 mL). The reaction was stirred at room temperature for 2 h, then diluted in water (100 mL) and extracted with ethyl acetate (2 × 50 mL). The organic solution was dried over Na₂SO₄, and the solvent was removed under reduced pressure. The residue was purified by silica gel chromatograph using 1:1 ethyl acetate/hexanes for afford **37** (0.6 g) in 78% yield as white solid (mp. 118.0-120.0 °C). ¹HMR (CD₃Cl, 300 MHz) δ 7.66 (s, 1H), 6.63 (s, 1H), 4.15 (m, 1H), 2.81-2.65 (m, 2H), 2.32 (s, 3H), 1.52 (s, 9H), 1.24 (d, 3H, *J* = 6.0 Hz).

1-(6-(*tert*-Butoxycarbonylamino)-4-methylpyridin-2-yl)propan-2-yl methanesulfonate (38)

Into a solution of **37** (0.25 g, 0.94 mmol) was added triethyl amine (200 μL, 1.44 mmol), followed by methanesulfonyl chloride (80 μL, 1.0 mmol). The reaction mixture was stirred at room temperature for 1 h, then diluted with water (20 mL). The product was extracted with CH₂Cl₂ (2 × 50 mL), and the combined organic layer was dried over Na₂SO₄. After removal of the solvent under reduced pressure, the residue was purified by silica gel chromatograph using 1:2 ethyl acetate/hexanes to afford **38** (0.27 g) in 83% yield as white solid (mp. 61-63 °C). ¹HMR (CD₃Cl, 300 MHz) δ 7.66 (s, 1H), 6.69 (s, 1H), 5.16 (m, 1H), 3.03-2.82 (m, 2H), 2.62 (s, 3H), 2.31 (s, 3H), 1.52 (s, 9H), 1.48 (d, 3H, *J* = 6.3 Hz).

Radiosynthesis of [¹⁸F]9

~180 mCi [¹⁸F]fluoride was dried by azeotropic distillation using CH₃CN (3 × 1 mL) in the presence of K₂CO₃ (0.75 mg) and K₂₂₂ (5 mg) at 110 °C under a flow of N₂, then a solution of **38** (2.5 mg) in CH₃CN (400 μL) was added. After the reaction mixture was heated in an oil bath (110 °C) for 10 min [incorporation: 17.3 ± 4.4% (n = 10) according to radio-TLC analysis: silica, 1:1 ethyl acetate/hexanes], it was passed through a silica gel SepPak (Waters) and CH₃CN (2 × 1 mL) was used to rinse the reaction vial and the SepPak. The elution was concentrated to less than 500 μL in the presence of 1N HCl (100 μL) at 110 °C under a flow of N₂, then 1N HCl (500 μL) was added. The reaction mixture was irradiated under microwave for 30 and 25 sec with an interval of 30 sec between each irradiation, and then was diluted in water (3 mL) for HPLC injection. [¹⁸F]9 was purified by reversed phased HPLC using an Alltech Platinum EPS C18 column (250 × 10 mm, 10 μ) eluted with 15% CH₃CN, 85% water with 0.1% trifluoroacetic acid (TFA) at a flow rate of 4 mL/min and UV at 272 nm. The radioactivity (~8 mCi) corresponding to [¹⁸F]9 was collected at 17 min, and the collection fraction was concentrated under reduced pressure to less than 0.5 mL and then diluted in water (40 mL). [¹⁸F]9 was separated from the dilution by passing the dilution through an Oasis HLC cartridge (Waters) and eluted from the cartridge with ethanol (1~2 mL). If necessary, the ethanol solution was concentrated under a flow of N₂ in order to make a final dose for animal study with <10% ethanol in saline. The total synthesis and purification time was 120 min; decay-corrected radiochemical yield was 6.2 ± 2.1% (n = 10); Radiochemical purity was >99.9% and specific activity was 2,160 ± 1,660 mCi/μmol (n = 10) at the end of synthesis, analyzed by an analytical HPLC column (Alltech Platinum EPS C18 250 × 4.6 mm, 10μ, 20% CH₃CH, 80% water, 0.1% TFA, 2 mL/min, 272 nm) and determined by comparison of the integrated UV absorbance with a calibrated mass/UV absorbance curve of **9**. The identity of

[¹⁸F]**9** was confirmed by the coelution of [¹⁸F]**9** with nonradioactive standard **9** on the analytical HPLC system.

NOS Enzyme Assays

All assays were performed using the Nitric Oxide Synthase Screening Kit (GE Healthcare Biosciences Corp., Piscataway, NJ) following the manufacturer's protocol with minor modifications. Recombinant inducible nitric oxide synthase (iNOS), endothelial nitric oxide synthase (eNOS), and neuronal nitric oxide synthase (nNOS) (Cayman Chemical Company, Ann Arbor, MI) were assayed to establish optimal enzyme concentrations and conditions. In short, all assays were carried out in reaction buffer containing 50 mM Tris pH 7.4, 1.0 mM NADPH, 3.8 μM FMN, 3.8 μM FAD, 3.8 μM tetrahydro-L-biopterin, 2.0 mM dithiothreitol, and 2.0 μM L-arginine, with the exception of the eNOS and nNOS assays which included 20 μg/mL calmodulin and 1 mM CaCl₂ in the reaction buffer to stabilize the enzymes. All chemicals used in the reaction buffer were purchased from EMD Chemicals Inc. (Gibbstown, NJ). Assays were performed at 80 μL per well in 96-well format. All experimental inhibitors were diluted in methanol or water to ensure compatibility with the assay. 100,000 cpm or 0.1 μCi [³H]Arginine was added to the enzyme-inhibitor mixture to initiate the reaction. The reaction was allowed to incubate for 30 min at room temperature before it was terminated by the addition of 40 μL Yttrium-Silicate SPA Arginine binding beads in 'stop solution' (50 mg/mL in 50 mM NaOH solution). The arginine binding beads were allowed to settle for 2 h before the plates were counted on a Micro-Beta (PerkinElmer Life and Analytical Sciences, Waltham, MA). Inhibition curves were determined using Kaleidagraph (Synergy Software, Reading, PA). All IC₅₀ values were recorded as mean ± S.D. (N ≥ 3).

Western Blot Analysis

Lungs from non-treated and LPS-treated C57BL/6N mice (Charles River Laboratories, Wilmington MA) were harvested and homogenized in T-Per® tissue protein extraction reagent (Pierce Biotechnology, Rockford, IL) containing Complete™ protease Inhibitor cocktail tablets (Roche Applied Science, Indianapolis, IN) on ice. Homogenates were sonicated 5-10 seconds 3 times on ice and centrifuged at 12,000 rpm at 4 °C for 15 min. Aliquots of protein (200 μg) from each sample were analyzed using standard immunoblotting procedures. The presence of iNOS was probed with monoclonal anti-iNOS primary antibody (Sigma-Aldrich, Inc., St. Louis, MO) at a 1:1,000 dilution and horseradish peroxidase-conjugated goat anti-rabbit IgG (Cell Signaling Technology, Danvers, MA) at 1:3,000 dilution. The SuperSignal WestDura Extended Duration Substrate assay kit (Pierce Biotechnology, Rockford, IL) was used to detect the secondary antibody. Loading control was performed with β-actin (Cell Signaling Technology, Danvers, MA).

In vitro stability study

An *in vitro* stability study was carried out in heparinized whole rat blood (mature male Sprague-Dawley rat). The whole blood (5 mL) was incubated with ~400 μCi [¹⁸F]**9** in 150 μL saline for 5 min, 30 min, 1 h and 2 h at 37 °C. An aliquot of blood was treated with 3 volumes of ethanol at each time point, and the lysed sample was centrifuged to separate the supernatant from the pellet. The radioactivity in the supernatant and the pellet was counted separately on a Beckman Gamma 8000 well counter. The radioactive species in the supernatant was analyzed by Silica TLC using ethyl acetate as the developing solvent (R_f = 0.7 for [¹⁸Br]**9**) and co-elution with non-radioactive **9**.

In vivo blood metabolism study

The metabolism of [¹⁸F]**9** was evaluated in a male Sprague-Dawley rat by iv injection of [¹⁸F]**9** (400 μCi) in 10% ethanol/saline via the tail vein of an anesthetized rat. Blood samples (1.2

mL) were obtained via cardiac puncture under anesthesia at 5 and 30 min post-injection. The plasma was separated from the red blood cells by centrifugation (14,000 rpm), and the radioactivity in both samples was measured. After the plasma (400 μ L) was treated with 3 equivalents of acetonitrile, supernatant and pellet were separated by centrifugation (14,000 rpm) and the radioactivity in both samples was measured. The supernatant was filtered through a 0.45 μ m nylon filter, and acetonitrile (1 mL) was used to rinse the filter. This supernatant solution was concentrated under a flow of N₂ at room temperature to less than 400 μ L. The radioactive species in the supernatant was analyzed by silica gel radio-TLC (developed in ethyl acetate and co-spotted with non-radioactive **9**) and reverse phase HPLC (co-eluted with **9**). All the samples were kept on ice to prevent degradation.

***In vivo* biodistribution time-course study**

All animal experiments were conducted in compliance with the Guidelines for the Care and Use of Research Animals established by Washington University's Animal Studies Committee. The biodistribution study was performed in mature male C57BL/6N mice (age 6-8 weeks) in two experimental groups: one group was intravenously injected with lipopolysaccharide (LPS) (*Escherichia coli* O127:B8, Sigma-Aldrich Co., MO) dissolved in PBS (10 mg/kg, μ L per mouse, i.v.) 6 h prior to the tracer injection to induce iNOS expression; untreated mice were used as control. Reverse phase HPLC purified [¹⁸F]**9** was injected (~50 μ Ci in 120 μ L 10% ethanol/saline, i.v.) via the tail vein. At the specified time points post-injection (5 min, 30 min, 1 h, and 2 h), the mice were sacrificed, and blood, tissues, and organs were removed, weighed, and counted in a Beckman Gamma 8000 counter with standard diluted aliquots of the injectate. The percent injected dose per gram of tissue (%ID/g) was presented as mean \pm standard deviation.

The blocking study was performed following the same procedure described above with the addition of a blocking group (injected with 1400W, 5 mg/kg in saline, i.v.). [¹⁸F]**9** was injected (~5 μ Ci in 120 μ L 10% ethanol/saline, i.v.) via the tail vein. Based on the tracer uptake profile exhibited in the initial biodistribution study and the kinetics of the blocking agent, uptake was evaluated 1 hour post-injection. A lower dose of [¹⁸F]**9** with higher specificity (4,300 mCi/ μ mol) was used in this study than in the initial evaluation.

MicroPET study

Two groups of mature male C57BL/6N mice (age 6-8 weeks) were used for the MicroPET study: one set was intratracheally injected with LPS (*Escherichia coli* O127:B8, Sigma-Aldrich Co., MO, 10 mg/kg) 6 h prior to the tracer injection (n=2); the other set received no treatment and was used as control (n=2). The mice were anesthetized with isoflurane and injected with ~100 μ Ci/100 μ L of [¹⁸F]**9** via the tail vein. The imaging sessions were carried out as 1 h dynamic scan using the MicroPET[®] Focus (Siemens Medical Solutions USA, Inc.) scanner. The MicroPET data was then processed using filter back projection algorithm with attenuation and scatter corrections.

Supplementary Material

Refer to Web version on PubMed Central for supplementary material.

Acknowledgments

This research was supported by the National Institute of Health grants HL13851 and CA 86307.

a Abbreviations:

NO, nitric oxide

NOS, nitric oxide synthase
 iNOS, inducible nitric oxide synthase
 eNOS, endothelial nitric oxide synthase
 nNOS, neuronal nitric oxide synthase
 LPS, lipopolysaccharide
 PET, positron emission tomography
 DAST, diethylaminosulfur trifluoride
 PBSF, perfluorobutane sulfonyl fluoride
 SEITU, S-ethylisothiourea
 L-NIL, L-N⁶-(1- iminoethyl)lysine
 2-AP, 2-aminopyridine

References

- 1 (a). For the latest reviews, see: Mollace V, Muscoli C, Masini E, Cuzzocrea S, Salvemini D. Modulation of prostaglandin biosynthesis by nitric oxide and nitric oxide donors. *Pharmacol. Rev* 2005;57:217–252. [PubMed: 15914468] (b) Alderton WK, Cooper CE, Knowles RG. Nitric oxide synthases: structure, function and inhibition. *Biochem. J* 2001;357:593–615. [PubMed: 11463332]
- 2 (a). Stuehr DJ. Mammalian nitric oxide synthases. *Biochim. Biophys. Acta* 1999;1411:217–30. [PubMed: 10320659] (b) Marletta MA. Nitric oxide synthase structure and mechanism. *J. Biol. Chem* 1993;268:12231–12234. [PubMed: 7685338]
- 3 (a). Marletta MA, Hurshman AR, Rusche KM. Catalysis by nitric oxide synthase. *Curr. Opin. Chem. Biol* 1998;2:656–663. [PubMed: 9818193] (b) Alderton WK, Cooper CE, Knowles RG. Nitric oxide synthases: structure, function and inhibition. *Biochem. J* 2001;357:593–615. [PubMed: 11463332]
4. Nathan C. Nitric oxide as a secretory product of mammalian cells. *FASEB J* 1992;6:3051–3064. [PubMed: 1381691]
- 5 (a). Titheradge MA. Nitric oxide in septic shock. *Biochim. Biophys. Acta* 1999;1411:437–455. [PubMed: 10320674] (b) Hobbs AJ, Higgs A, Moncada S. Inhibition of nitric oxide synthase as a potential therapeutic target. *Annu. Rev. Pharmacol. Toxicol* 1999;39:191–220. [PubMed: 10331082] (c) Vallance P, Leiper J. Blocking NO synthesis: how, where and why? *Nat. Rev. Drug Discov* 2002;1:939–950. [PubMed: 12461516] (d) Moore DJ, West AB, Dawson VL, Dawson TM. Molecular pathophysiology of Parkinson's disease. *Annu. Rev. Neurosci* 2005;28:57–87. [PubMed: 16022590] (e) Li H, Förstermann U. Nitric oxide in the pathogenesis of vascular disease. *J. Pathol* 2000;190:244–254. [PubMed: 10685059] (f) Xu W, Liu LZ, Loizidou M, Ahmed M, Charles IG. The role of nitric oxide in cancer. *Cell Res* 2002;12:311–320. [PubMed: 12528889]
6. Lechner M, Lirk P, Rieder J. Inducible nitric oxide synthase (iNOS) in tumor biology: the two sides of the same coin. *Semin. Cancer Biol* 2005;15:277–289. [PubMed: 15914026]
- 7 (a). Narayanan K, Spack L, McMillan K, Kilbourn RG, Hayward MA, Masters BS, Griffith OW. S-Alkyl-L-thiocitrullines. Potent stereoselective inhibitors of nitric oxide synthase with strong pressor activity in vivo. *J. Biol. Chem* 1995;270:11103–11110. [PubMed: 7538112] (b) Moore WM, Webber RK, Jerome GM, Tjoeng FS, Misko TP, Currie MG. L-N⁶-(1-iminoethyl)lysine: a selective inhibitor of inducible nitric oxide synthase. *J. Med. Chem* 1994;37:3886–3888. [PubMed: 7525961] (c) Moore WM, Webber RK, Fok KF, Jerome GM, Connor JR, Manning PT, Wyatt PS, Misko TP, Tjoeng FS, Currie MG. 2-Iminopiperidine and other 2-iminoazaheterocycles as potent inhibitors of human nitric oxide synthase isoforms. *J. Med. Chem* 1996;39:669–672. [PubMed: 8576908] (d) McCall TB, Feelisch M, Palmer RM, Moncada S. Identification of N-iminoethyl-L- ornithine as an irreversible inhibitor of nitric oxide synthase in phagocytic cells. *Br. J. Pharmacol* 1991;102:234–238. [PubMed: 1710525] (e) Furfine ES, Harmon MF, Paith JE, Knowles RG, Salter M, Kiff RJ, Duffy C, Hazelwood R, Oplinger JA, Garvey EP. Potent and selective inhibition of human nitric oxide synthases. Selective inhibition of neuronal nitric oxide synthase by S-methyl-L-thiocitrulline and S-ethyl-L-thiocitrulline. *J. Biol. Chem* 1994;269:26677–26683. [PubMed: 7523410] (f) Narayanan K, Spack L, McMillan K, Kilbourn RG, Hayward MA, Masters BS, Griffith OW. S-Alkyl-L- thiocitrullines. Potent stereoselective inhibitors of nitric oxide synthase with strong pressor activity in vivo. *J. Biol. Chem* 1995;270:11103–11110. [PubMed: 7538112] (g) Southan GJ, Szabo

- C, Thiemermann C. Isothioureas: potent inhibitors of nitric oxide synthases with variable isoform selectivity. *Br. J. Pharmacol* 1995;14:510–516. [PubMed: 7533622]
- 8 (a). Young RJ, Beams RM, Carter K, Clark HA, Coe DM, Chambers CL, Davies PI, Dawson J, Drysdale MJ, Franzman KW, French C, Hodgson ST, Hodson HF, Kleanthous S, Rider P, Sanders D, Sawyer DA, Scott KJ, Shearer BG, Stocker R, Smith S, Tackley MC, Knowles RG. Inhibition of inducible nitric oxide synthase by acetamidine derivatives of hetero-substituted lysine and homolysine. *Bioorg. Med. Chem. Lett* 2000;10:597–600. [PubMed: 10741561] (b) Garvey EP, Oplinger JA, Furfine ES, Kiff RJ, Laszlo F, Whittle BJ, Knowles RG. 1400W is a slow, tight binding, and highly selective inhibitor of inducible nitric-oxide synthase in vitro and in vivo. *J. Biol. Chem* 1997;272:4959–4963. [PubMed: 9030556] (c) Strub A, Ulrich WR, Hesslinger C, Eltze M, Fuchss T, Strassner J, Strand S, Lehner MD, Boer R. The novel imidazopyridine 2-[2-(4-methoxy-pyridin-2-yl)-ethyl]-3H-imidazo[4,5-b]pyridine (BYK191023) is a highly selective inhibitor of the inducible nitric-oxide synthase. *Mol. Pharmacol* 2006;69:328–337. [PubMed: 16223957] (d) Beaton H, Hamley P, Nicholls DJ, Tinker AC, Wallace AV. 3,4-Dihydro-1-isoquinolinamines: a novel class of nitric oxide synthase inhibitors with a range of isoform selectivity and potency. *Bioorg. Med. Chem. Lett* 2001;11:1023–1026. [PubMed: 11327580] (e) Naka M, Nanbu T, Kobayashi K, Kamanaka Y, Komeno M, Yanase R, Fukutomi T, Fujimura S, Seo HG, Fujiwara N, Ohuchida S, Suzuki K, Kondo K, Taniguchi N. A potent inhibitor of inducible nitric oxide synthase, ONO-1714, a cyclic amidine derivative. *Biochem. Biophys. Res. Commun* 2000;270:663–667. [PubMed: 10753680]
- 9 (a). Faraci WS, Nagel AA, Verdries KA, Vincent LA, Xu H, Nichols LE, Labasi JM, Salter ED, Pettipher ER. 2-Amino-4-methylpyridine as a potent inhibitor of inducible NO synthase activity in vitro and in vivo. *Br. J. Pharmacol* 1996;119:1101–1108. [PubMed: 8937711] (b) Pettipher ER, Hibbs TA, Smith MA, Griffiths RJ. Analgesic activity of 2-amino-4-methylpyridine, a novel NO synthase inhibitor. *Inflamm. Res* 1997;46:S135–S136. [PubMed: 9297548]
10. Hagmann WK, Caldwell CG, Chen P, Durette PL, Esser CK, Lanza TJ, Kopka IE, Guthikonda R, Shah SK, MacCoss M, Chabin RM, Fletcher D, Grant SK, Green BG, Humes JL, Kelly TM, Luell S, Meurer R, Moore V, Pacholok SG, Pavia T, Williams HR, Wong KK. Substituted 2-aminopyridines as inhibitors of nitric oxide synthases. *Bioorg. Med. Chem. Lett* 2000;10:1975–1978. [PubMed: 10987430]
11. Connolly S, Aberg A, Arvai A, Beaton HG, Cheshire DR, Cook AR, Cooper S, Cox D, Hamley P, Mallinder P, Millichip I, Nicholls DJ, Rosenfeld RJ, StGallay SA, Tainer J, Tinker AC, Wallace AV. 2-Aminopyridines as highly selective inducible nitric oxide synthase inhibitors. Differential binding modes dependent on nitrogen substitution. *J. Med. Chem* 2004;47:3320–3323. [PubMed: 15163211]
- 12 (a). Zhang J, McCarthy TJ, Moore WM, Currie MG, Welch MJ. Synthesis and evaluation of two positron-labeled nitric oxide synthase inhibitors, S-[¹¹C]methylisothiourea and S-(2-[¹⁸F]fluoroethyl)isothiourea, as potential positron emission tomography tracers. *J. Med. Chem* 1996;39:5110–5118. [PubMed: 8978842] (b) Tian H, Lee Z. Radiosynthesis of 8-fluoro-3-(4-[¹⁸F]fluorophenyl)-3,4-dihydro-1-isoquinolinamine ([¹⁸F]FFDI), a potential PET radiotracer for the inducible nitric oxide synthase. *Current Radiopharmaceuticals* 2008;1:49–53. (c) de Vries EF, Vroegh J, Dijkstra G, Moshage H, Elsinga PH, Jansen PL, Vaalburg W. Synthesis and evaluation of a fluorine-18 labeled antisense oligonucleotide as a potential PET tracer for iNOS mRNA expression. *Nucl. Med. Biol* 2004;31:605–612. [PubMed: 15219279]
13. Peterson DJ. Carbonyl olefination reaction using silyl-substituted organometallic compounds. *J. Org. Chem* 1968;33:780–784.
14. Bryk R, Wolff DJ. Pharmacological modulation of nitric oxide synthesis by mechanism-based inactivators and related inhibitors. *Pharmacol. Ther* 1999;84:157–178. [PubMed: 10596904]
15. Tiso M, Strub A, Hesslinger C, Kenney CT, Boer R, Stuehr DJ. BYK191023 (2-[2-(4-methoxy-pyridin-2-yl)-ethyl]-3h-imidazo[4,5-b]pyridine) is an NADPH- and time-dependent irreversible inhibitor of inducible nitric-oxide synthase. *Mol. Pharmacol* 2008;73:1244–1253. [PubMed: 18178668]
16. Speyer CL, Neff TA, Warner RL, Guo RF, Sarma JV, Riedemann NC, Murphy ME, Murphy HS, Ward PA. Regulatory effects of iNOS on acute lung inflammatory responses in mice. *Am. J. Pathol* 2003;163:2319–2328. [PubMed: 14633605] (a) Liu SF, Adcock IM, Old RW, Barnes PJ, Evans TW. Differential regulation of the constitutive and inducible nitric oxide synthase mRNA by lipopolysaccharide treatment in vivo in the rat. *Crit. Care Med* 1996;24:1219–1225. [PubMed:

- 8674339] (b) Buttery LD, Evans TJ, Springall DR, Carpenter A, Cohen J, Polak JM. Immunochemical localization of inducible nitric oxide synthase in endotoxin-treated rats. *Lab Invest* 1994;7:755–764. [PubMed: 7526041] (c) Kan W, Zhao KS, Jiang Y, Yan W, Huang Q, Wang J, Qin Q, Huang X, Wang S. Lung, spleen, and kidney are the major places for inducible nitric oxide synthase expression in endotoxic shock: role of p38 mitogen-activated protein kinase in signal transduction of inducible nitric oxide synthase expression. *Shock* 2004;21:281–287. [PubMed: 14770043]
17. Moncada S, Higgs EA. Molecular mechanisms and therapeutic strategies related to nitric oxide. *FASEB J* 1995;9:1319–1330. [PubMed: 7557022]
- 18 (a). Kovách AG, Szabó C, Benyó Z, Csáki C, Greenberg JH, Reivich M. Effects of NG-nitro-L-arginine and L-arginine on regional cerebral blood flow in the cat. *J. Physiol* 1992;449:83–196. (b) Benyó Z, Kiss G, Szabó C, Csáki C, Kovách AG. Importance of basal nitric oxide synthesis in regulation of myocardial blood flow. *Cardiovasc. Res* 1991;25:700–703. [PubMed: 1913760] (c) Gardiner SM, Compton AM, Bennett T, Palmer RM, Moncada S. Control of regional blood flow by endothelium-derived nitric oxide. *Hypertension* 1990;15:486–492. [PubMed: 2332239]
19. Alderton WK, Angell AD, Craig C, Dawson J, Garvey E, Moncada S, Monkhouse J, Rees D, Russel RJ, Schwartz S, Waslidge N, Knowles RG. GW274150 and GW273629 are potent and highly selective inhibitors of inducible nitric oxide synthase in vitro and in vivo. *Br. J. Pharmacol* 2005;145:301–312. [PubMed: 15778742]
20. Newman, Melvin S.; Waltcher, I.; Ginsberg, HF. The synthesis and reduction of some polyfunctional acetylene compounds. *J. Org. Chem* 1952;17:962–970.

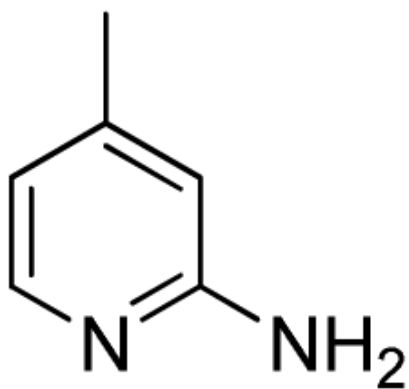
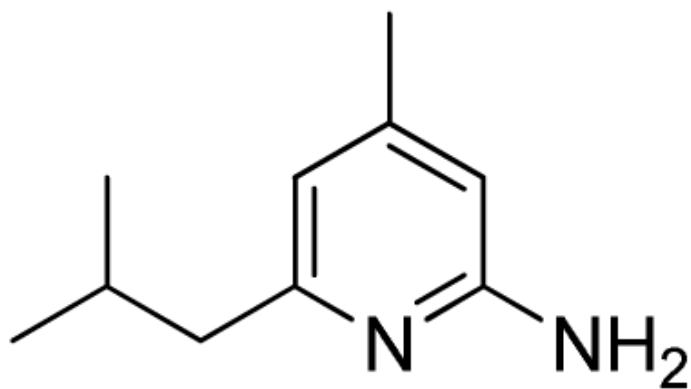
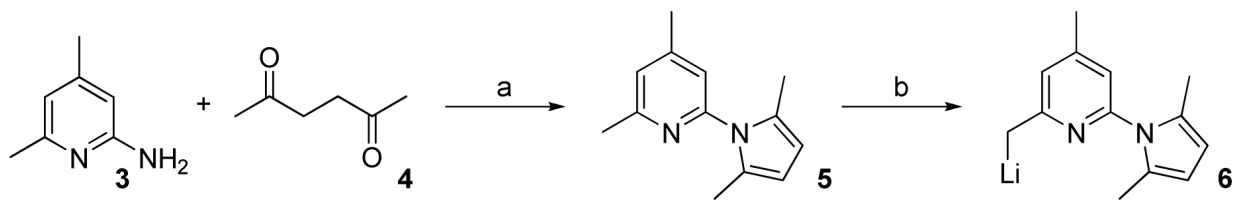
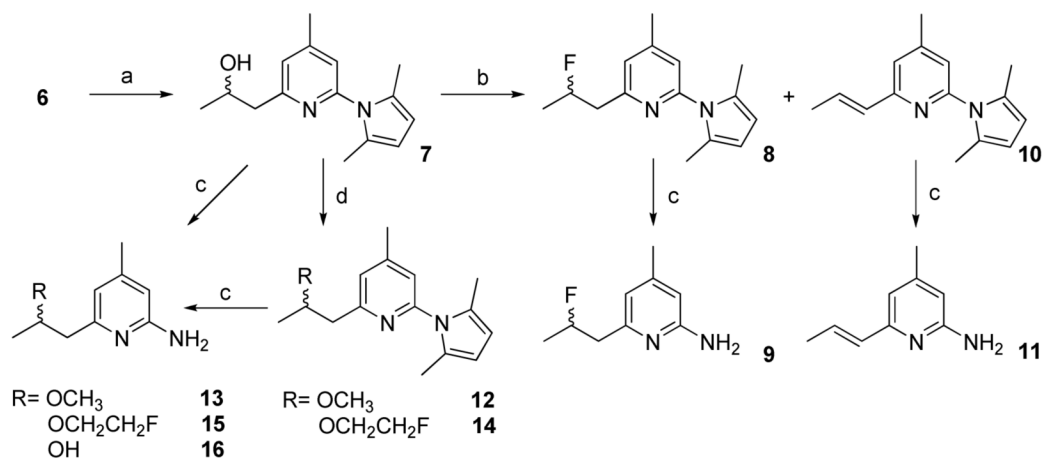
**1**

Chart.

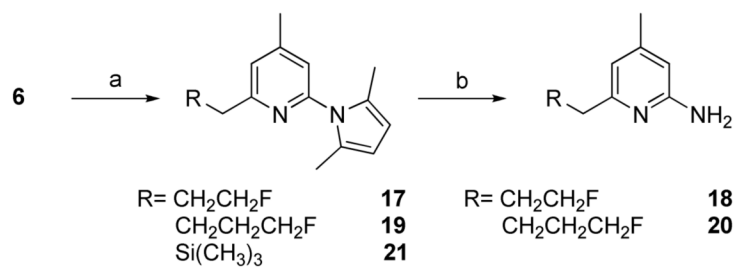
**2**

**Scheme 1.**

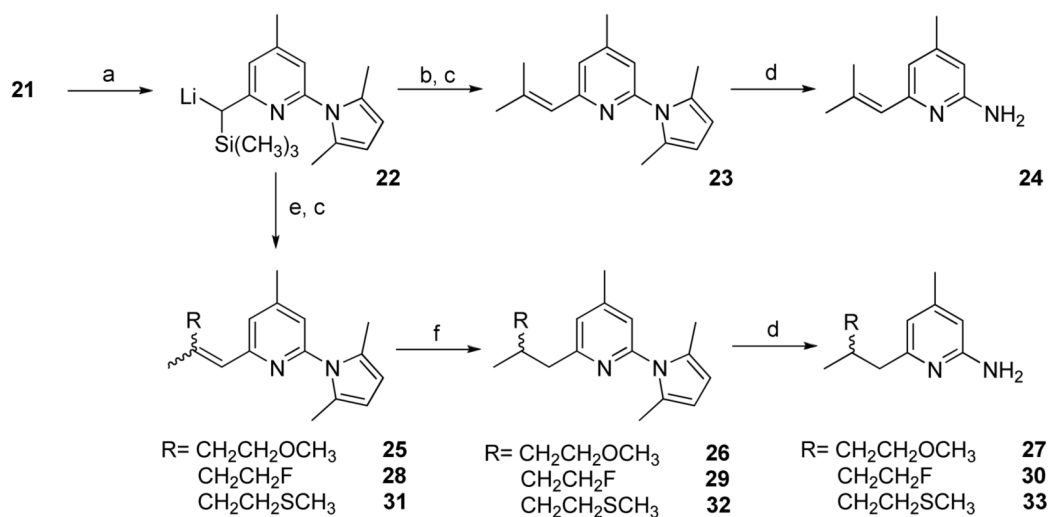
Reagents and conditions: (a) HOAc, Toluene, reflux; (b) *n*-BuLi, Et₂O, -20 to -10 °C.

**Scheme 2.**

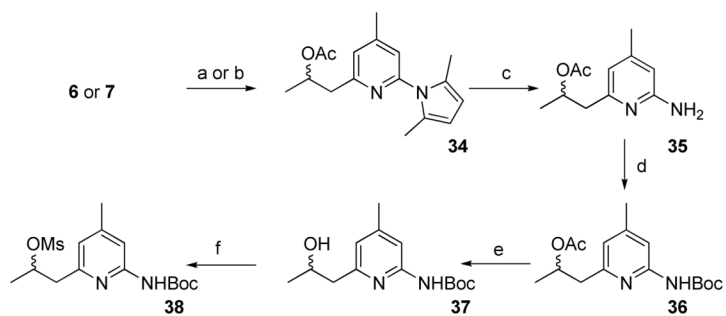
Reagents and conditions: (a) CH_3CHO , Et_2O , -78°C to RT; (b) DAST, CH_2Cl_2 or PBSF, $(\text{NEt}_3)(\text{HF})_3$, Et_3N , CH_3CN ; (c) $\text{NH}_2\text{OH}\cdot\text{HCl}$, EtOH , H_2O ; (d) CH_3I or $\text{BrCH}_2\text{CH}_2\text{F}$, NaH , THF .

**Scheme 3.**

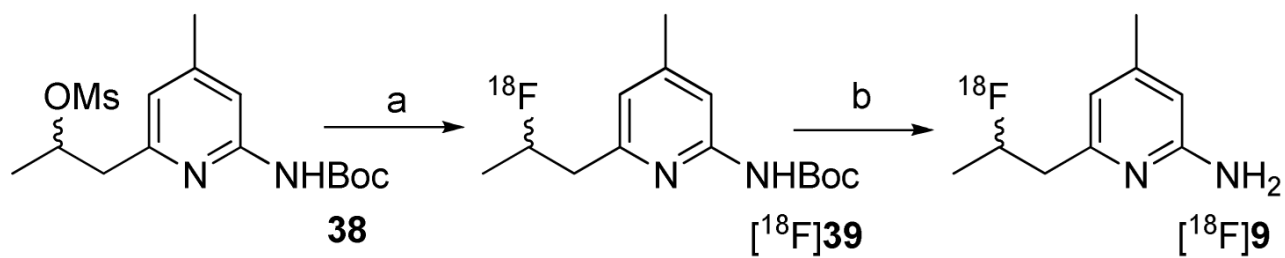
Reagents and conditions: (a) **17**: BrCH₂CH₂F or **19**: BrCH₂CH₂CH₂F or **21**: (CH₃)₃SiCl, Et₂O; (b) NH₂OH·HCl, EtOH, H₂O.

**Scheme 4.**

Reagents and conditions: (a) *n*-BuLi, Et₂O, -20 °C; (b) acetone, Et₂O, -78 °C to RT; (c) 1N HCl; (d) NH₂OH·HCl, EtOH, H₂O; (e) **25**: CH₃COCH₂CH₂OCH₃; **28**: CH₃COCH₂CH₂F; or **31**: CH₃COCH₂CH₂SCH₃, Et₂O, -78 °C to RT; (f) HCOONH₄, Pd/C, H₂, EtOH, 80 °C (**25**, **28**); or Mg, EtOH (**31**).

**Scheme 5.**

Reagents and conditions: (a) **6**: CH₃CHO, Et₂O, -78 °C to RT; then AcOEt, Et₂O; (b) **7**: AcCl, Et₃N, CH₂Cl₂; (c) NH₂OH·HCl, EtOH, H₂O; (d) Boc₂O, *t*-BuOH; (e) K₂CO₃, MeOH, H₂O; (f) MsCl, Et₃N, CH₂Cl₂

**Scheme 6.**

Reagents and conditions: (a) $[^{18}\text{F}]$ fluoride, K_2CO_3 , K_{222} , CH_3CN , $110\text{ }^\circ\text{C}$; (b) 1N HCl , microwave.

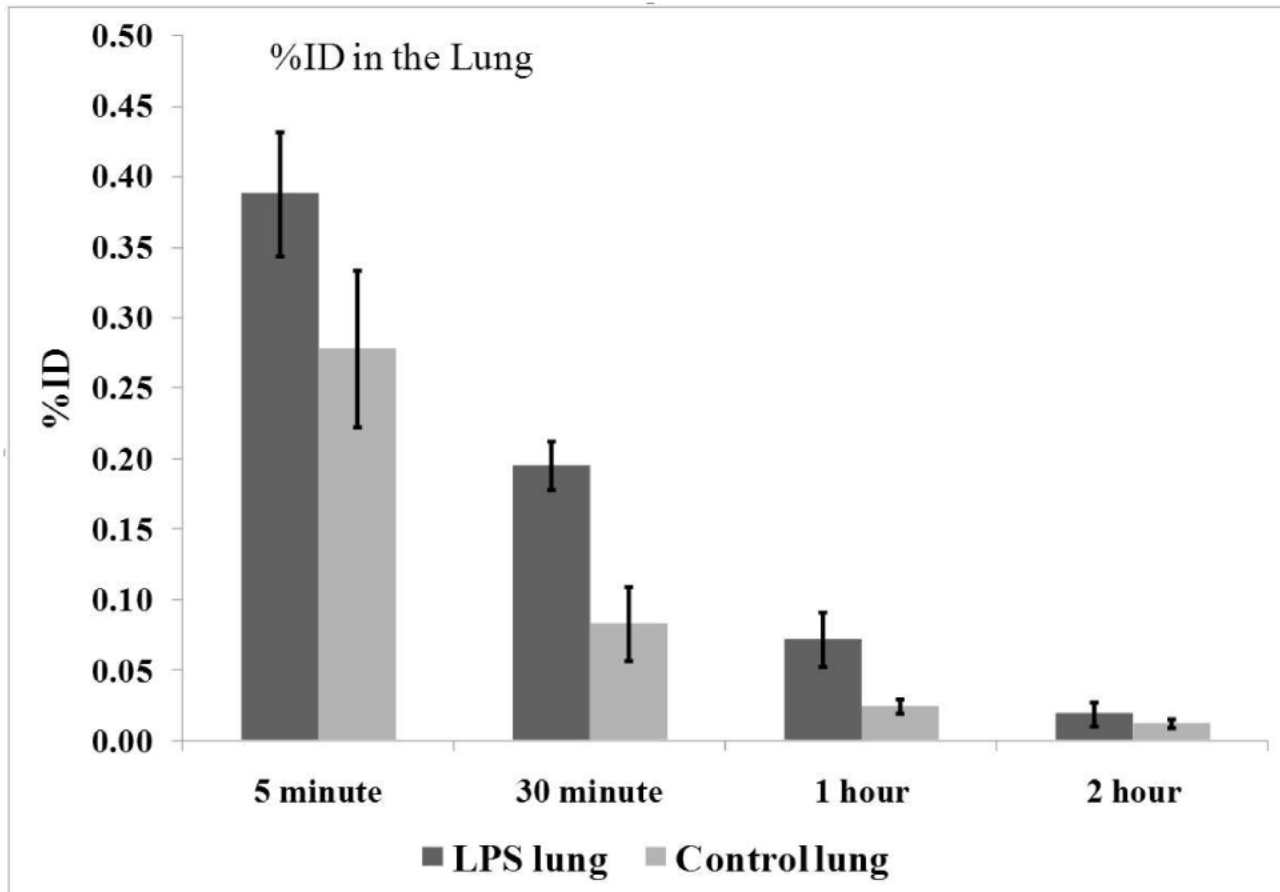


Figure 1. Comparison of total lung activity post-injection of [^{18}F]9 in LPS-pretreated mice vs. control mice.

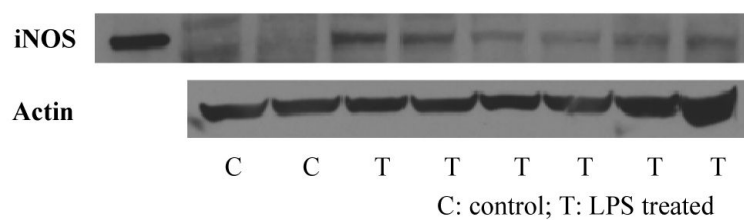


Figure 2. Representative Western blots showing the levels of iNOS expression in lungs from the control and LPS treated mice. The first lane is purified iNOS as a positive control (iNOS); no iNOS expression was observed in the lungs of normal mice (C); different degrees of iNOS expression were found in the lungs of the LPS-treated mice (T).

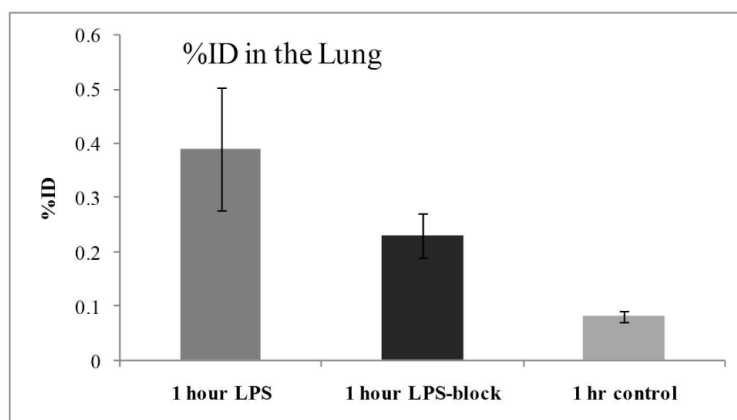


Figure 3. Comparison of activity in the lung 1 h post-injection of [^{18}F]**9** in the control, LPS treated, and LPS-treated-1400W-blocked mice (mean %ID/g \pm SD, $n = 4$, $p < 0.05$)

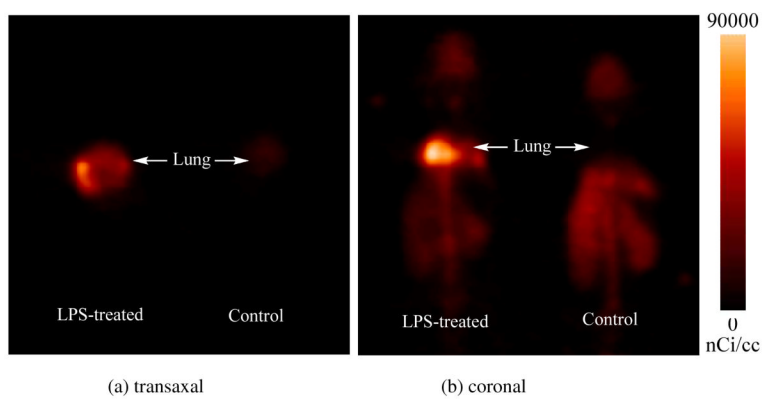
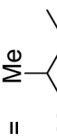
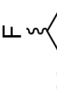
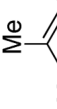
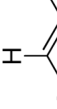
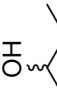

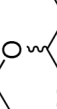


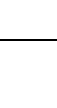
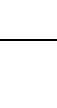
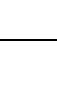
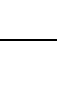
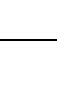


Figure 4. Whole-body MicroPET images of [^{18}F]9 in the LPS-treated mice (left) and the control mice (right). (a) transaxal, (b) coronal. Images were summed from 0 to 60 min after injection of [^{18}F]9. Accumulation of the activity was observed in the lungs of the LPS-treated mouse, whereas no such accumulation in the normal control.

Table 1

IC₅₀ values of the 2-Amino-4-Methylpyridine analogs^a

NOS	R=													
														
	2	9	24	11	16	13	15	18	20	27	30	30	27	33
iNOS	193±38 (28) ^c	220±25	685±127	282±49	1776±395	>5000	>5000	57.6±5.3	170±26	-	731±87	-	>5000	>5000
eNOS	(150) ^c	1500±300	^d	-	-	-	-	1428±158	-	-	-	-	-	-
nNOS	(100) ^c	490±80	-	-	-	-	-	514±83	-	-	-	-	-	-

^aNote: Using recombinant human iNOS, eNOS and nNOS

^bStandard iNOS IC₅₀ [measured (reported)]: SEITU = 30.5±4.6 (32), L-NIL = 1465±148 (1400), 2-AP = 108±35 (170)

^cref. 10

^d“^c” not determined.

Table 2

Biodistribution of [^{18}F]9 in control vs. LPS treated mice^a (data reported as mean %ID/g \pm SD; n = 4)^b

%ID/g	5 min		30 min		1 h		2 h	
	LPS	Control	LPS	Control	LPS	Control	LPS	Control
Blood	3.69 \pm 0.38	2.37 \pm 0.18	2.09 \pm 0.35	1.22 \pm 0.16	0.86 \pm 0.09	0.31 \pm 0.04	0.23 \pm 0.05	0.27 \pm 0.22
Lung	4.32 \pm 0.32	3.33 \pm 0.28	1.84 \pm 0.27	1.14 \pm 0.13	0.73 \pm 0.17	0.31 \pm 0.06	0.18 \pm 0.09	0.15 \pm 0.03
Liver	24.6 \pm 3.1	33.2 \pm 3.3	7.06 \pm 0.28	10.7 \pm 0.3	2.63 \pm 0.52	2.59 \pm 0.49	0.42 \pm 0.15	0.74 \pm 0.23
Kidney	26.7 \pm 4.1	20.6 \pm 2.4	10.9 \pm 2.8	7.30 \pm 0.66	3.95 \pm 0.53	2.20 \pm 0.25	0.91 \pm 0.63	0.80 \pm 0.27
Muscle	1.64 \pm 0.09	1.25 \pm 0.06	1.06 \pm 0.40	0.71 \pm 0.31	0.78 \pm 0.47	0.27 \pm 0.18	0.23 \pm 0.13	0.34 \pm 0.27
Heart	2.03 \pm 0.06	1.50 \pm 0.12	1.02 \pm 0.16	0.60 \pm 0.05	0.41 \pm 0.10	0.19 \pm 0.02	0.12 \pm 0.04	0.08 \pm 0.02
Brain	1.81 \pm 0.09	1.60 \pm 0.17	0.52 \pm 0.15	0.28 \pm 0.02	0.19 \pm 0.03	0.11 \pm 0.02	0.07 \pm 0.03	0.07 \pm 0.03
Bone	1.59 \pm 0.15	1.52 \pm 0.36	3.70 \pm 1.20	2.26 \pm 0.55	4.30 \pm 0.90	2.57 \pm 0.64	3.77 \pm 1.41	5.59 \pm 4.20

^aNote: LPS mice were treated with lipopolysaccharide (LPS) 10 mg/kg i.v. 6 h prior to tracer injection; all mice were injected with 50 $\mu\text{Ci}/110 \mu\text{L}$ [^{18}F]9

^bSD: standard deviation.